Topographic Influences on the Path of the Gulf Stream[1]

By BRUCE A. WARREN, *Woods Hole Oceanographic Institution, Woods Hole, Massachusetts*

(Manuscript received November 9, 1962, revised version March 29, 1963)

ABSTRACT

Meander patterns observed in the Gulf Stream east of Cape Hatteras exhibit correlations with bottom topography. An examination of the orders of magnitude of terms in the Gulf Stream vorticity balance suggests that if the current extends to the ocean bottom, as implied by some recent deep velocity measurements, its path must indeed be controlled principally by the topography of the Continental Rise, with a generally smaller constraint imposed by the meridional variation of the Coriolis parameter. Approximate current paths calculated according to this mechanism—steady-state conservation of potential vorticity—agree sufficiently well with observed paths to confirm the topographic explanation of large-scale meanders.

The observed variety in meander patterns is attributed to fluctuations in current direction and path curvature near Cape Hatteras.

These conclusions make doubtful any direct relation between large-scale meanders and possible instabilities of the Gulf Stream east of Cape Hatteras, and between the distribution of wind stress and the separation of Stream from coast.

1. Introduction

It has been generally assumed in recent years that meanders in the Gulf Stream represent amplified perturbations to some fairly uniform, unstable current (HAURWITZ and PANOFSKY, 1950; STOMMEL, 1958, pp. 129–131; STERN, 1961). Although the difficulties in integrating equations with variable coefficients have prohibited stability analyses of current models having sufficient complexity to resemble the actual Gulf Stream, the wave-like character of observed meander patterns has made explanations based on instability hypotheses very appealing.

The few long, fairly well determined current paths actually observed east of Cape Hatteras, however, exhibit certain correlations with the trend of isobaths on the Continental Rise. This circumstance, while not conclusive, suggests a topographic influence on the path of the Stream, and makes pertinent a dynamical inquiry into the possibility and nature of such an effect. A study is therefore undertaken here of the vorticity balance typically satisfied in these paths. The analysis reveals that a convincing description of their gross features can be given in terms of the constraint exerted by sloping bottom topography on a quasi-geostrophic current which extends to the bottom of the ocean; with generally minor modifications imposed by the meridional variation in Coriolis parameter. The analysis suggests, moreover, that only this mechanism is quantitatively sufficient to account for these features. Thus it appears that the meanders in the Gulf Stream east of Cape Hatteras are not associated with unstable waves after all, but are segments of topographically controlled stable waves, analogous to stationary Rossby waves (ROSSBY, 1940).

2. Topographic correlations with observed current paths

Several surveys of the Gulf Stream have served to chart nearly synoptic segments of its path east of Cape Hatteras. These studies have been greatly facilitated through the role played by the Stream as the boundary between the Sargasso Sea and the slope water (ISELIN, 1936), for the Stream position can be conveniently located according to the pronounced horizontal difference in properties between the two water masses. Five path segments have been defined with sufficient precision in this manner, over sufficiently long distances, to make compari-

[1] Contribution No. 1326 from the Woods Hole Oceanographic Institution.

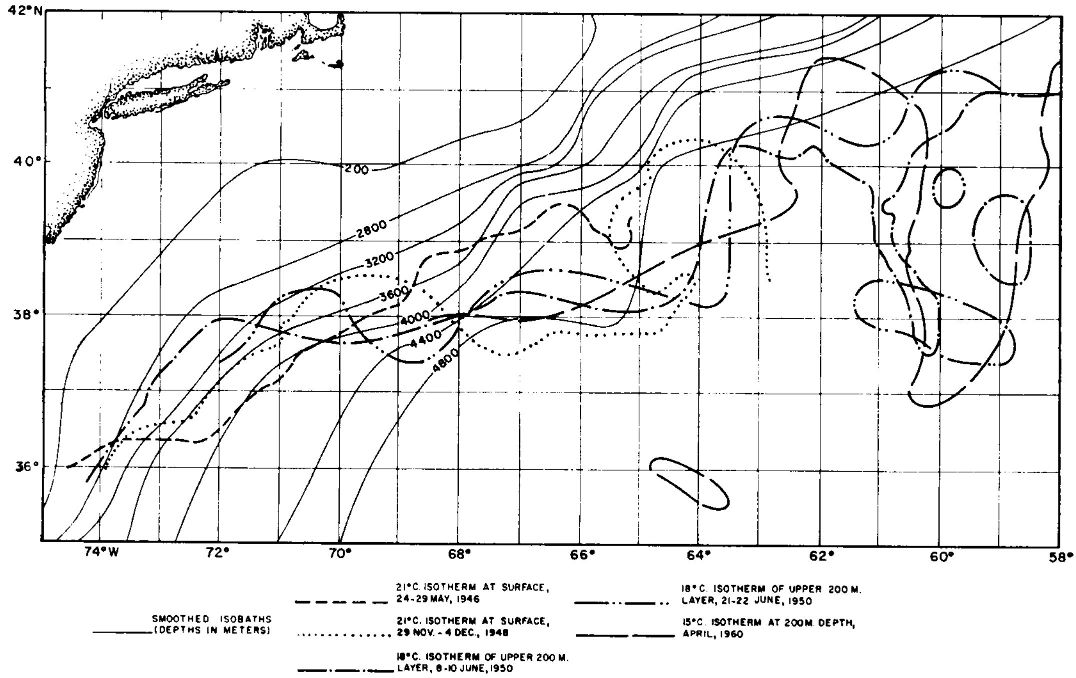

FIG. 1. Observed paths of the Gulf Stream overlying smoothed bottom topography. Isotherms from articles cited in the text are used as path indicators.

sions potentially informative. Each one is indicated in Fig. 1 by the positions at some depth of an isotherm lying in the center of the sharp horizontal temperature gradient characteristic of the Stream. These curves are based on figures included in articles to be cited below. The variety in path indicators is unfortunate, but was imposed by the variety in nature of the source material.

The two earliest current paths are both represented in Fig. 1 by surface positions of the 21°C isotherm. The relevant observational data consist of many short, closely spaced, bathythermograph sections made in late May 1946, on board the *Atlantis* (FUGLISTER and WORTHINGTON, 1947; ISELIN and FUGLISTER, 1948), and in late November and early December 1948, on the *New Liskeard* (FORD and MILLER, 1952).

Bathythermograph sections were again used to locate the Stream during a multiple-ship survey in June 1950 (FUGLISTER and WORTHINGTON, 1951). The paths taken by the Stream at the beginning (8–10 June) and the end (21–22 June) of the survey are shown by the positions of the 18°C isotherm of the upper 200 m layer. As may be seen in the figure, a long, narrow, cyclonic meander, which was discovered early in the survey, broke away from the Stream to form an eddy, while an eddy east of the meander moved to the northwest, and diminished in size.

On a much longer multiple-ship survey, made in the spring of 1960 (FUGLISTER, in press), sections were run along meridians spaced two degrees (about 180 km) apart. The temperature data obtained are the basis for the current path indicated in Fig. 1 by the positions of the 15°C isotherm at the 200 m level. Although observations were separated by distances considerably greater than in the previous surveys mentioned, the interpolation was generally confirmed by electromagnetic "lines of zero-set" (VON ARX, 1960). Ambiguity remains concerning possible connections between the great cyclonic meander and the eddy southwest of it; that portion of the current path, however, has no particular importance in the present study.

A span of fourteen years thus separates the earliest from the most recent path observation.

One should remember, however, that the two paths of 1950 are separated by only two weeks.

Fig. 1 includes a very rough representation of bottom topography in the general area of these surveys. The isobaths are based on U.S. Coast and Geodetic Survey chart No. 1000 (14th ed., revised as of 20 March 1961) and U.S. Navy Hydrographic Office chart No. 6610-L (1st ed., revised as of 24 October 1960); they are shown in highly smoothed form, because it was felt that to have superposed detailed current paths on detailed isobaths would have obscured the general trend of the deep topography, the feature of significance to this discussion. The coastline and 200 m curve roughly define the limits of the Continental Shelf; seaward to a depth of about 2000 m lies the Continental Slope; the deep isobaths, increasing in depth at 400 m intervals from 2800 to 4800 m, depict the general shape of the Continental Rise. The depth of the Abyssal Plain is about 5000–5200 m. For clarity, the New England Seamounts, located east of longitude 65°W, have been omitted from the figure. Other topographic features seaward of the 4800 m curve are comparatively insignificant.

Clearly, although the Gulf Stream no longer presses against the Continental Slope after it passes Cape Hatteras, it by no means enters directly onto the Abyssal Plain, but approaches it only after flowing for more than a thousand kilometers over the Continental Rise. Probably the most striking characteristic common to the current paths in this region is one pointed out by FUGLISTER (in press): that the downstream amplification of their meanders does not occur gradually, but abruptly at longitudes 65°–62° W, where the four current paths which extend that far east turn abruptly northward and subsequently develop great anticyclonic meanders. It is noteworthy that in these same longitudes there exists a similar bend in the deep bottom contours. A curious feature of these four meanders, moreover, is that the envelope of their crests coincides to a remarkable degree with the 4600 m isobath. Far upstream, furthermore, the general trend of current paths is northeastward, similar to that of the isobaths, and where the bottom contours bend rather sharply eastward, near longitudes 71°–69° W, so also does the trend of current paths.

Although these correlations are somewhat tenuous, they suggest that bottom topography may provide a control on the path of the Gulf Stream which is involved fundamentally in the dynamics of meanders. Such a notion would certainly be frivolous were it in fact true, as was for so long assumed, that the deep water of the ocean is virtually motionless. Recent temperature and salinity profiles, however, have revealed that the horizontal density gradient associated with the Stream, and indicative of vertical shear of horizontal motion, persists down to the bottom of the ocean, although with considerable reduction in magnitude from its thermocline value (see, for instance, FUGLISTER, 1960). On the other hand, direct observations of deep motions beneath the surface Gulf Stream are rather sparse, and those relevant to the Stream east of Cape Hatteras are nearly limited to Fuglister's survey of 1960 (FUGLISTER, in press). On that occasion, neutrally buoyant Swallow floats were set out in deep water directly beneath the surface Stream, and followed for several days. At the same time the float tracks were bracketed with pairs of hydrographic stations. By integrating vertically the horizontal density gradient obtained from the station data, and using the measured float velocity as a constant of integration, curves of geostrophic velocity with depth could then be calculated. These showed a Gulf Stream which extended to the bottom of the ocean without reversing direction, and with bottom velocities averaging about 8–10 cm/sec. Hence present evidence, though sparse, indicates the existence of deep flow in the Gulf Stream, through which topographic features could conceivably influence the current path at all depths.

3. The vorticity balance of the meandering Stream

We are thus prompted to examine the full equation of motion for a significant topographic effect which could account for these correlations. An analysis of the orders of magnitude of its various terms has therefore been undertaken for numbers typical of the Gulf Stream east of Cape Hatteras. Unfortunately, present inadequate knowledge of time variations precludes completely satisfactory assessments of certain terms. Nevertheless, what information is presently available suggests a very simple gross vorticity balance: namely, steady-state conservation of potential vorticity. The actual analysis is too lengthy to be included here, but will be sketched briefly; the details may be found elsewhere (WARREN, 1962).

To a first approximation, Gulf Stream velocities are proportional to the cross-stream pressure gradients. Since it is the small departures from this proportionality which are crucial to meandering motions, however, it is desirable for present purposes to eliminate the first-order balance by studying not the momentum equation itself, but the vertical component of its curl, the vorticity equation:

$$\frac{\partial \zeta}{\partial t} + \nabla \cdot (\zeta + f)\mathbf{V} - \nabla \cdot w(2\mathbf{\Omega} + \nabla \times \mathbf{V}) + \mathbf{k} \cdot \nabla\alpha \times \nabla p - \mathbf{k} \cdot \nabla \times \mathbf{F} = 0. \quad (1)$$

The symbols are defined as:

- $\mathbf{V}$ —water velocity relative to the earth, with horizontal and vertical components, $\mathbf{V}_H$ and w
- ∇ —gradient operator, with horizontal component, ∇_H
- $2\mathbf{\Omega}$—twice the angular velocity of the earth, with vertical component, f (the Coriolis parameter)
- $\mathbf{k}$ —vertical unit vector, directed upward
- ζ —vertical component of relative vorticity, equal to $\mathbf{k} \cdot \nabla \times \mathbf{V}$
- t —time
- α —specific volume
- p —pressure
- $\mathbf{F}$ —frictional force per unit mass

We approximate the meridional variation of the Coriolis parameter in the usual way by retaining only the constant and linear terms of its Taylor series expansion. Thus if x, y, and z denote a local Cartesian reference frame, with coordinates increasing eastward, northward, and upward respectively, then we represent $f(y)$ as: $f = f_0 + \beta y$, where f_0 is the value of the parameter at some latitude in the area under study, and β is the corresponding value of df/dy.

We supplement (1) with the approximate form of the continuity equation,

$$\nabla \cdot \mathbf{V} = 0. \quad (2)$$

In order to remove terms pertaining only to the internal current structure, and not to the position of the Stream as a whole, it proves useful to integrate (1) over a volume R fixed in space, which spans the entire width of the current, and extends from the sea surface to the top of the frictional boundary layer at the ocean bottom. The bounding surface of R is to be composed of six subsurfaces: two nearly vertical surfaces respectively parallelling each side of the current, but lying outside the concentrated flow; two nearly vertical surfaces crossing the current at arbitrary points to connect the first pair, but so shaped and oriented as to be normal to the flow; a nearly horizontal surface lying along the sea surface; and another nearly horizontal surface, lying just above the bottom frictional boundary layer. Let the bottom surface be designated by B, and the pair of vertical surfaces which cross the current, by S. Further, let an integral over S be understood as the sum of integrals over both members of S.

The velocity field in the Gulf Stream and its environment has as yet been only partially described. Fortunately, only a crude representation is required. We consider a jet-like current having a total volume transport V of the order 10^{14} cm-sec^{-1} (one hundred million cubic meters per second); a total transport of momentum per unit mass M of the order 5×10^{15} cm^4-sec^{-2}; and a volume transport per unit depth near the ocean bottom T of the order 10^8 cm^2-sec^1. That these are reasonable numbers by which to characterize the Stream is seen in noting that they describe approximately a jet 125 km wide, with a triangular cross-stream velocity profile whose maximum decreases linearly with depth from a surface value of 160 cm-sec^{-1} to a 1200 m value of 16 cm-sec^{-1}; and subsequently remains constant down to an ocean bottom at a depth of 4500 m. This current has a cross-stream averaged bottom velocity of 8 cm-sec^{-1}, consonant with the calculations pertaining to portions of the Gulf Stream in 1960.

Little is known either of the slow, over-all time changes in the Stream path which determine the volume integral of the first term of (1), or of the smaller-scale fluctuations which determine the fifth term through Reynolds stresses. There is some basis, however, for supposing both effects small in comparison with those represented by the second and third terms of (1). The most extensive and least ambiguous observations of changes in a meander pattern are those of the 1950 multiple-ship survey. On that occasion, the meanders moved downstream and changed shape, both events apparently occurring at about the same rate (except in the immediate vicinity of the detaching cyclonic meander). Therefore we can gain some idea of the relative importance of the first term in (1) simply by considering a meander pattern in which time changes are due solely to translation at some constant speed of the pattern as a whole. For such a speed equal to 5 cm-sec^{-1}—appropriate to the observations of both 1950 and 1960—the volume integral of $\partial\zeta/\partial t$ turns out not to be significant. Hence we omit the term from the gross vorticity balance.

Even less is known of the mixing processes producing eddy stresses. It has been a common practice to represent such stresses in terms of eddy coefficients and mean gradients—a practice admitted unsatisfactory, especially so for ocean currents since WEBSTER (1961*a*) calculated, in effect, negative coefficients for portions of the Florida Current. For lack of anything else, however, probably eddy coefficients can be used to give rough indications of the general magnitude of turbulent effects. On this basis we should require a horizontal coefficient greater than 10^8 cm^2-sec^{-1} to have a significant frictional contribution to the integrated vorticity balance. While such values may characterize the climatological-mean Stream, the few estimates made for fluctuations of much shorter period (those therefore pertinent to the quasi-synoptic Stream, the object of present concern) are much smaller. Thus Webster's surface-velocity calculations would give coefficients of order 10^6–10^7 cm^2-sec^{-1}, while STOMMEL (1955) calculated values of order 10^5–10^6 cm^2-sec^{-1} from certain surface-velocity measurements of Pillsbury in the Florida Straits. With reservations, then, we disregard friction.

Oceanic density variations are much too small to permit a significant solenoid effect (fourth term of eq. (1)).

It seems likely, therefore, that the integrated vorticity balance of the Gulf Stream east of Cape Hatteras (far from the Continental Slope) essentially derives only from the second and third terms of (1). With suitable transformations of volume integrals into surface integrals, it is expressed approximately as:

$$\int_S (Kv + \beta y)\, \mathbf{V}_H \cdot \mathbf{n}\, d\sigma + f_0 \int_{BH} w_T\, d\sigma = 0. \qquad (3)$$

K is the horizontal streamline curvature (of order 10^{-2} km^{-1}); v, the magnitude of $\mathbf{V}_H$; $\mathbf{n}$, a unit normal to S, directed out of R; and $d\sigma$, an element of surface area. (Relative vorticity is expressed here as the sum of the cross-stream velocity shear and the product Kv; since velocities are small outside the Stream, the shear makes only a negligible contribution to the total vorticity transport.) Surface BH is the horizontal projection of B, and w_T is the "topographic component" of the vertical velocity at B, imposed by a sloping bottom. Since the upper surface of the bottom frictional boundary layer must closely parallel the bottom topography, we may write w_T as $-\mathbf{V}_{HB} \cdot \nabla D$, where $\mathbf{V}_{HB}$ is the value of $\mathbf{V}_H$ at B, and D represents the ocean depth, counted positive (w_T is then of order 5×10^{-2} cm-sec^{-1}). Apparently, then, the Gulf Stream is indeed subject to a significant topographic effect, as conjectured above.

Eq. (3) actually asserts that, in an integrated sense, the Gulf Stream exhibits steady-state conservation of potential vorticity: it describes a very simple meander mechanism, composed of two dynamical features. The curvature and β-terms by themselves would describe a stationary Rossby wave: a current of constant volume transport, flowing northward over a level bottom cannot remain in geostrophic balance, for the northward increase in Coriolis parameter, coupled with the condition of constant transport, implies a gradual increase in magnitude of the Coriolis force acting on the current over that of the pressure gradient force. The net force produced imparts an acceleration normal to the direction of flow, resulting in eastward deflection of the current, and the development of anticyclonic curvature in the streamlines. The deflective force and curvature increase until the direction of flow becomes due east; as the current continues to turn, now to the south, the force diminishes, and finally vanishes when the current returns to its original latitude, where exact geostrophy is again established. The anticyclonic meander so formed is then followed by a cyclonic meander, since continued southward motion leads to a deflective force of opposite sense to that above.

The curvature and topographic terms alone in (3) would describe a "topographic wave", associated with a similar imbalance between Coriolis and pressure gradient forces. The conservation of volume transport in a current which extends to the bottom of the ocean requires a redistribution of velocity as the current flows over a shoaling bottom: if the current maintains its width, the velocity at all levels must increase, and hence—for constant Coriolis parameter—the Coriolis force acting on the current also; if the current broadens, so that velocities need not increase for the current to maintain its transport, the cross-stream pressure gradient must decrease. In any case, just as in the Rossby wave, there must occur a relative increase in Coriolis over pressure gradient force, and an attendant development of anticyclonic curvature. Similarly, a development of cyclonic curvature must be associated with flow over a deepening bottom, so that again the current executes a sinuous path. Whereas the axes of Rossby waves lie along parallels of latitude, the axes of these topographic waves must be related to the trend of the isobaths. The meandering current described by eq. (3), then, represents a certain combination of these two stationary waves.

We might remark parenthetically that, although at first glance a topographic effect achieved through such forced variations in the depth of a quasi-geostrophic current would seem to be required also in a current which does not extend to the ocean bottom, but has a sloping surface of no horizontal motion as a lower boundary (NEUMANN, 1956), eq. (3) shows that this cannot be so. Since the effect due to the slope of the lower boundary is proportional to the horizontal velocity on it, if that boundary is a surface of *zero* horizontal velocity, the "topographic" influence must vanish. Closer scrutiny reveals that the two superficially similar situations are in fact fundamentally different. In a quasi-geostrophic current, the cross-stream pressure gradient must vanish on a surface of no horizontal motion; consequently, if that surface deepens in the downstream direction, the cross-stream pressure gradient must increase downstream along all levels above the surface. Therefore there must exist a pressure-gradient component parallel to the main current along at least one side of it, and a corresponding geostrophic flow into the current across that lateral boundary. Thus the depth variation of a current flowing above a sloping surface of no motion does not imply a redistribution of velocity tending to destroy geostrophic equilibrium, but simply a gradual change in the volume transport of the main current.

4. Approximate current paths

To see now whether the large-scale meander patterns of Fig. 1 are actually explicable in terms of steady-state conservation of potential vorticity, it becomes desirable to compute current paths as determined by eq. (3), and compare them with the observed paths. With a further specification of volume R, and a set of credible approximations, it is possible to transform (3) from a sum of integrals into a tractable, ordinary differential equation useful for such computations. Integration over S in (3) involves two surfaces, which we shall designate S_1 and S_2. Let the upstream surface S_1 be fixed to cross the current at an inflection in its path, so that

$$\int_{S_1} K v \mathbf{V}_H \cdot \mathbf{n} d\sigma = 0.$$

Furthermore, let the origin of the coordinate system (x, y) be set in S_1 at such a position that

$$\int_{S_1} x \mathbf{V}_H \cdot \mathbf{n} d\sigma = \int_{S_1} y \mathbf{V}_H \cdot \mathbf{n} d\sigma = 0.$$

On S_2 (where $\mathbf{V}_H$ is normal to $\mathbf{n}$) we define weighted average values of x, y, and K—indicated by bars—according to the relations:

$$\int_{S_2} x \mathbf{V}_H \cdot \mathbf{n} d\sigma \equiv \bar{x} \int_{S_2} v d\sigma = \bar{x} V,$$

$$\int_{S_2} y \mathbf{V}_H \cdot \mathbf{n} d\sigma \equiv \bar{y} \int_{S_2} v d\sigma = \bar{y} V,$$

$$\int_{S_2} K v \mathbf{V}_H \cdot \mathbf{n} d\sigma \equiv \bar{K} \int_{S_2} v^2 d\sigma = \bar{K} M,$$

so that by a current path we shall now mean a curve $\bar{y}$ $(\bar{x})$. In addition, we identify the curvature of $\bar{y}$ $(\bar{x})$ with $\bar{K}$ by making the assumption:

$$K \cong \frac{d^2\bar{y}}{d\bar{x}^2}\left[1+\left(\frac{d\bar{y}}{d\bar{x}}\right)^2\right]^{-\frac{3}{2}}. \quad (4)$$

The other approximations bear on the topographic term. For convenience we define natural horizontal coordinates (l, a) based on the streamlines of $\mathbf{V}_{HB}$, such that l measures distance along streamlines, in the direction of $\mathbf{V}_{HB}$, and a, distance normal to them.
Then

$$\int_{BH} w_T d\sigma = -\int_{BH} \mathbf{V}_{HB}\cdot\nabla_H D d\sigma = -\int_{BH} v_B \frac{\partial D}{\partial l}\, dl da,$$

where v_B is the magnitude of $\mathbf{V}_{HB}$. Since, as may be seen in Fig. 1, we are concerned with depth changes which are small compared with the total ocean depth, we may regard the divergent part of $\mathbf{V}_{HB}$ as small compared with the non-divergent part, and take

$$\int_{BH} v_B \frac{\partial D}{\partial l}\, dl da \cong \int v_B \delta D da, \quad (5)$$

where the integration over a is between the lateral bounds of the current, and δD denotes the change in depth along a streamline of $\mathbf{V}_B$ between the cross-stream boundaries of surface B: B_1 and B_2, which lie in surfaces S_1 and S_2. Furthermore, we define a weighted cross-stream average of δD by the relation,

$$\int v_B \delta D da \equiv \overline{\delta D}\int v_B da = \overline{\delta D} T.$$

For analytic convenience we shall approximate the actual, curved ocean bottom by a system of planes with slopes and orientations appropriate to the local topography. Accordingly, we represent δD as

$$\delta D = D_x(x_2 - x_1) + D_y(y_2 - y_1),$$

where (x_1, y_1) are the coordinates of a streamline of $\mathbf{V}_B$ on B_1, and (x_2, y_2) are the corresponding coordinates on B_2; the parameters D_x and D_y are the locally averaged x and y components of $\nabla_H D$. The essence of this plane approximation is that we treat D_x and D_y locally as constants, but also as parameters which change their values discontinuously from one region of the Continental Rise to another.

We relate $\overline{\delta D}$ to $\bar{y}$ $(\bar{x})$ by making the additional assumptions,

$$\int_{B_1} x v_B da \cong \int_{B_1} y v_B da \cong 0,$$

$$\int_{B_2} x v_B da \cong \bar{x}\int_{B_2} v_B da = \bar{x}T,$$

$$\int_{B_2} y v_B da \cong \bar{y}\int_{B_2} v_B da = \bar{y}T,$$

where $\bar{x}$ and $\bar{y}$ are defined as above. The basic assumption here is that the bottom current is not very much out of phase with the vertically averaged current, nor laterally displaced very much from it. Thus

$$\overline{\delta D} \cong D_x\bar{x} + D_y\bar{y}. \quad (6)$$

If we now insert these representations into eq. (3), we obtain a non-linear, ordinary differential equation. For simplicity we shall henceforth omit the bars indicative of averages, but always understand the current path $y(x)$ to mean strictly the curve $\bar{y}(\bar{x})$ defined above. Thus,

$$\frac{d^2y}{dx^2}\left[1+\left(\frac{dy}{dx}\right)^2\right]^{-\frac{3}{2}} + Qy - Sx = 0, \quad (7)$$

where $Q \equiv (\beta V - f_0 T D_y)/M$ and $S \equiv f_0 T D_x/M$. For definiteness, we took the upstream surface S_1 to cross the current at the path inflection; were we instead to have the downstream surface S_2 cross at the inflection, we should simply change the sign of each term in (3), and hence not alter (7) at all. Thus eq. (7) describes a current path both upstream and downstream from the coordinate origin.

Strictly speaking, the coefficients in (7) vary along the current path, because the redistributions of velocity attendant on depth changes require variations in T and M. These, however, must be roughly proportional to the percentage changes in depth over meander quarter-wave lengths, which, as noted above, are fairly small. Furthermore, since it is roughly the ratio of T to M which appears in (7), the variations in coefficients must be smaller yet. Hence we treat (7) as having constant coefficients.

An immediate difficulty with (7) is its inhomogeneity. This is easily removed: it is clearly possible to transform the linear combination $Qy - Sx$ into a single term by an appropriate rotation of axes, and since curvature is an invariant property of a curve, the differentiated term must retain its form under such a transformation. Thus (7) is cast into the homogeneous form

$$\frac{d^2\eta}{d\xi^2}\left[1+\left(\frac{d\eta}{d\xi}\right)^2\right]^{-\frac{3}{2}}+P\eta=0, \tag{8}$$

where $P \equiv \sqrt{Q^2+S^2}$, by the rotation,

$$\left.\begin{aligned}\xi&=x\cos\theta+y\sin\theta,\\ \eta&=-x\sin\theta+y\cos\theta,\end{aligned}\right\} \tag{9}$$

in which $\theta \equiv \tan^{-1} S/Q$.

The proportionality between curvature and displacement shows clearly the oscillatory character of $\eta(\xi)$, which we of course expect from our interpretation of eq. (3). Equation (8) amounts to a generalization of an equation proposed by ROSSBY (1940) to describe, in effect, stationary Rossby waves; it reduces to Rossby's equation when $D_x = D_y = 0$. On the other hand, when $\beta = 0$, (8) describes a pure topographic wave. The structure of (8) is worth some attention, for it affords insight into the manner in which the Rossby and topographic waves combine to form the meandering current described by (3). The Rossby wave is characterized by the vector: $(V\nabla_H f)/M$, whose normal gives the direction of the wave axis, and whose magnitude measures the scale of the wave; the topographic wave for a plane ocean bottom is characterized in an identical fashion by the vector: $-(f_0 T\nabla_H D)/M$. Eq. (8) specifies the combination wave simply by the resultant of these two vectors; its normal defines the axis direction (θ), and its magnitude (P) is the scale parameter.

To obtain a first integral of (8) we make the substitution, $\eta'' = \eta' d\eta'/d\eta$, where primes indicate differentiation with respect to ξ. We prescribe the constant of integration by denoting the wave amplitude as η_0, i.e. we set $\eta^2 = \eta_0^2$ at $\eta' = 0$. Then integration of (8) yields:

$$P(\eta_0^2-\eta^2)-2[1-(1+\eta'^2)^{-\frac{1}{2}}]=0. \tag{10}$$

Thus for any value of η' formula (10) permits calculation of the associated value of η.

To find the corresponding value of ξ, we must perform another integration. We rewrite (10) in the form,

$$\left(\frac{d\xi}{d\eta}\right)^2=\frac{[1+P(\eta^2-\eta_0^2)/2]^2}{1-[1+P(\eta^2-\eta_0^2)/2]^2}, \tag{11}$$

from which it follows that

$$\xi=\int_0^\eta \frac{[1+P(\eta_0^2-\eta^2)/2]\,d\eta}{\sqrt{1-[1+P(\eta_0^2-\eta^2)/2]^2}}. \tag{12}$$

Any ambiguities in the sign of the integrand associated with extracting the square root of (11) are to be resolved by taking it consistent with the sign of $d\xi/d\eta$ in the range of integration. Since $\xi(\eta)$ is multi-valued, (11) cannot yield values of ξ in excess of a quarter-wave length of $\eta(\xi)$; such distances, therefore, are to be obtained by adding integral numbers of quarter-wave lengths to lesser distances calculated from (12).

Through an elliptic substitution, one can carry out the indicated integration, and express ξ in a form suitable for computations:

$$\xi=\frac{1}{\sqrt{P}}\left\{2E(\varphi,k)-F(\varphi,k)-\frac{k^2\sin^2\varphi}{\sqrt{1-k^2\sin^2\varphi}}\right\}, \tag{13}$$

where $F(\varphi, k)$ and $E(\varphi, k)$ are the elliptic integrals of the first and second kind, and

$$k^2=P\eta_0^2/4,$$

$$k^2\sin^2\varphi=\frac{P\eta^2/2}{2+P(\eta^2-\eta_0^2)/2}.$$

Although it is thus not possible to write the solution of (8) explicitly in the form: $\eta = \eta(\xi)$, nevertheless, given the direction of the current and curvature of its path at some point, eq. (8), (10), and (13) permit the calculation of any other point on a path described by (8). Then by inversion of formulas (9), one can find the corresponding points of the solution to (7).

5. Current path computations

In order to verify that steady-state conservation of potential vorticity can indeed account for the observed meander patterns of the Stream, an approximate current path, as formulated above, has been calculated to correspond to each Stream path shown in Fig. 1. Calculated paths were matched to observed paths by using the measured current direction

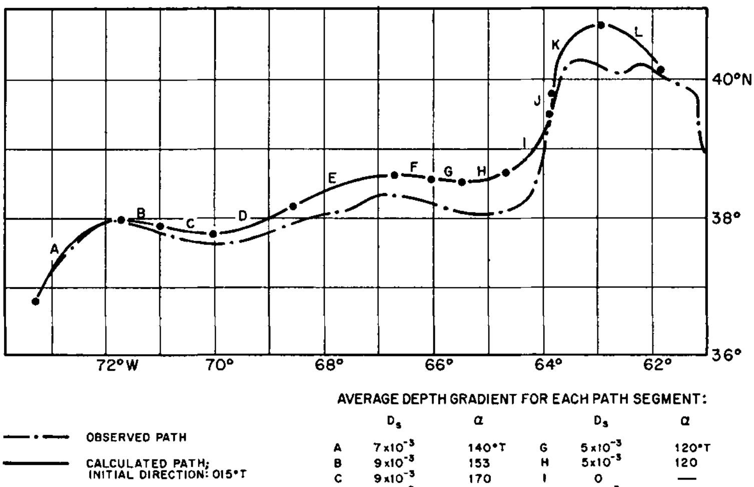

AVERAGE DEPTH GRADIENT FOR EACH PATH SEGMENT:

	D_s	α		D_s	α
A	7×10^{-3}	140°T	G	5×10^{-3}	120°T
B	9×10^{-3}	153	H	5×10^{-3}	120
C	9×10^{-3}	170	I	0	—
D	9×10^{-3}	170	J	7×10^{-3}	165
E	10×10^{-3}	165	K	7×10^{-3}	165
F	3×10^{-3}	135	L	7×10^{-3}	165

FIG. 2. Comparison of the Gulf Stream path observed on 8–10 June 1950 with a calculated current path matched to the observed path at its upstream end.

and path curvature at a single point on an observed path as the initial conditions required to determine a solution of eq. (7). Some care was necessary in choosing the initial points, because, while the observational data seem generally dense enough to permit estimating current directions with fair precision from the interpolated paths, they are much too sparse for correspondingly reliable estimates of path curvatures. On the other hand, they do allow rather close definition of the positions of path inflections. Therefore inflection points near the upstream ends of the observed path segments were adopted as initial points for all calculations.

Because considerable labor is involved in the repeated use of formulas (10) and (13), only the positions of selected points of particular interest on a current path were calculated: inflection points, relative maxima and minima in $y(x)$ or $\eta(\xi)$, infinities in dy/dx, or points at distinct boundaries between very different topographic regimes. A path was then drawn to connect these points from knowledge of the general character of solutions to eq. (8). The computational procedure was to guess the position of the first point of interest beyond the initial point, estimate the average value of $\nabla_H D$ over the connecting path segment, insert the value together with the current direction and path curvature at the initial point into (8), (10), and (13), and thus obtain coordinates (ξ, η) for the new point. By inverting (9), these were then translated into coordinates (x, y). If it happened that the estimated and calculated positions of the point were sufficiently different to make the depth-gradient value used in the calculation inappropriate to the topography actually underlying the calculated path segment, the procedure was repeated with revised values of $\nabla_H D$ until a self-consistent calculation was achieved. The computed path characteristics at this new point then served as initial conditions for calculating by the same procedure the position of the next desired point.

The values adopted for the current parameters V, M, and T were those used for the order-of-magnitude analysis outlined in Sect. 3, i.e. $V = 10^{14}$, $M = 5 \times 10^{15}$, $T = 10^{8}$ in c.g.s. units. (The same values were used in all calculations.) Since the latitudes concerned were roughly 36°–41° N, f_0 was taken as 0.9×10^{-4} sec^{-1}, and β, as $1.8 \times 10^{-13} \text{sec}^{-1}\text{-cm}^{-1}$. Values of $\nabla_H D$ were estimated from the bathymetric data presented on the charts cited in Sect. 2.

The five pairs of observed and calculated current paths are shown in Figs. 2–6. Solid lines denote calculated paths; the dots on them indicate the current positions actually computed. The dashed or dotted lines represent the observed paths as depicted in Fig. 1, and de-

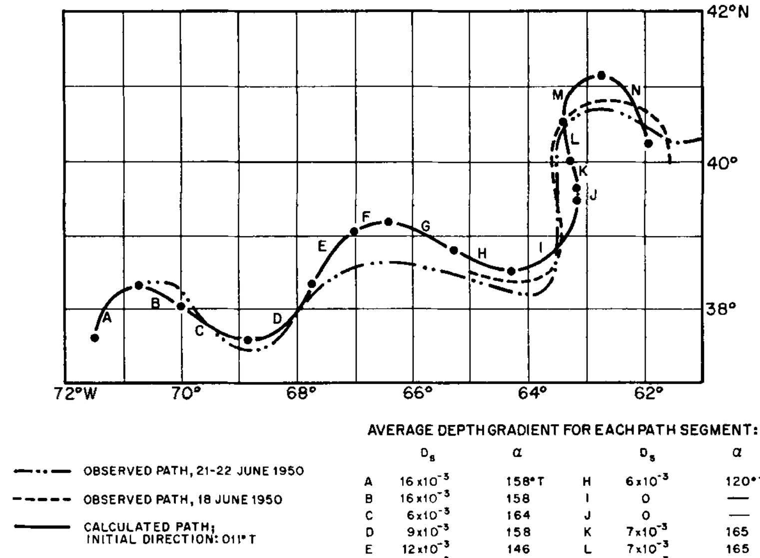

AVERAGE DEPTH GRADIENT FOR EACH PATH SEGMENT:

	D_s	α		D_s	α
A	16×10^{-3}	158°T	H	6×10^{-3}	120°T
B	16×10^{-3}	158	I	0	—
C	6×10^{-3}	164	J	0	—
D	9×10^{-3}	158	K	7×10^{-3}	165
E	12×10^{-3}	146	L	7×10^{-3}	165
F	12×10^{-3}	166	M	7×10^{-3}	165
G	4.5×10^{-3}	135	N	7×10^{-3}	165

FIG. 3. Comparison of the Gulf Stream path observed on 21–22 June 1950 with a calculated current path matched to the observed path at its upstream end. Also depicted is a segment of the path observed on 18 June 1950.

scribed in Sect. 2. The measured set of the current in degrees true at the initial inflection point (westernmost point of each path) is noted in the legend for every figure. The depth gradients used in the step-wise computations are given on the figures for each path segment by the magnitudes of the gradients D_s and their directions α in degrees true. (The computations were actually made in terms of linear distances between points, which were translated into angular coordinates by the relations appropriate to latitude 38° N: 1° of longitude = 88 km, 1° of latitude = 111 km.)

Fig. 2 has to do with the Gulf Stream path observed in early June 1950. Both it and the calculated path turn eastward near longitude 72° W, and meander very gently until they reach longitude 64° W, where they both turn abruptly northward and form large anticyclonic meanders. Downstream from the initial point the calculated path tends to run a little north of the observed path, but the agreement between the gross features of the two paths is very good.

The path taken by the Stream two weeks later is shown in Fig. 3. On 19 June the large cyclonic meander located near longitudes 61°–60° W (see Fig. 1) separated from the Stream. Since several assumptions employed in the derivation of eq. (7) must be invalid in the process of eddy formation, a calculated path probably ought strictly to be compared with the path observed just prior to separation rather than with that just after. Therefore a segment of the Stream path charted on 18 June (FUGLISTER and WORTHINGTON, 1951) is indicated on the figure by the positions of the 18°C isotherm of the upper 200 m layer. Both the observed and calculated paths in Fig. 3 meander much more vigorously upstream of longitude 64°W than those depicted in Fig. 2. Like the latter, they both turn abruptly northward at 64° W to form great anticyclonic meanders, but meanders of greater amplitude and smaller width than those of Fig. 2. The calculated path again tends to run a little north of the observed path, but the correspondence between gross features is as notable as above. The function $y(x)$ even becomes multi-valued between longitudes 64°–63° W, in agreement with the Stream path observed on 18 June.

These calculated patterns are easily understood qualitatively in terms of the distribution of isobaths. On the Continental Rise, the

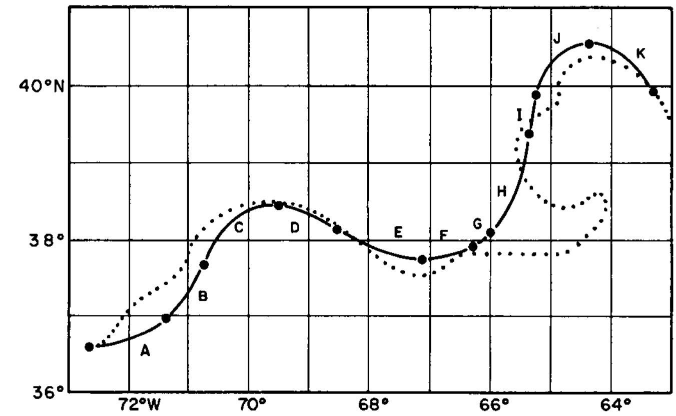

AVERAGE DEPTH GRADIENT FOR EACH PATH SEGMENT

	D_s	α		D_s	α
A	8×10^{-3}	130°T	G	4.5×10^{-3}	120°T
B	8×10^{-3}	142	H	4.5×10^{-3}	120
C	11×10^{-3}	153	I	7.5×10^{-3}	120
D	7×10^{-3}	165	J	7×10^{-3}	165
E	3×10^{-3}	155	K	7×10^{-3}	165
F	3×10^{-3}	155			

FIG. 4. Comparison of the Gulf Stream path observed 29 November–4 December 1948 with a calculated current path matched to the observed path at its upstream end.

contribution of the depth gradient term to the scale parameter P is three to six times greater than that of the β-term. Hence, upstream of longitude 64° W, the paths are guided by the topography in the manner described in Sect. 3: they meander about axes closely paralleling the isobaths. The amplitudes in late June exceed those in early June simply because the angle between the initial current direction and the trend of isobaths was greater for the former path than for the latter. Both paths inflect somewhat west of the abrupt northward turn in the deep bottom contours, and hence develop large cyclonic curvatures just as they leave the Continental Rise and pass onto the Abyssal Plain. The excess of pressure gradient over Coriolis force acting on the current is therefore relatively large at this point, and deflects the current to the north. Since the subsequent depth gradient is zero, the path becomes a segment of a stationary Rossby wave, subject only to the restoring effect of the variation in Coriolis parameter. Inasmuch as the β-effect is considerably weaker than the topographic effect experienced upstream, a correspondingly greater northward displacement is required to destroy the deflective tendency than was necessary before. In fact, the calculated currents do not actually inflect and turn eastward again until they are once more constrained by the Continental Rise, now found north of latitude 39°30′ N. Thus it is the abrupt bend in isobaths, permitting the currents to run onto the Abyssal Plain with relatively intense cyclonic curvature, which explains the development of the great anticyclonic meanders in the calculated paths.

On both occasions in 1950 the Gulf Stream displayed triple-crested meander patterns; in contrast, the 1948 pattern, shown in Fig. 4, is double-crested. Nevertheless the calculation reproduces the observed path with about the same fidelity that it did the 1950 paths. It does, however, miss the sharp indentation in the large anticyclonic meander. This discrepancy probably cannot be explained by weaknesses in the approximations used to transform (3) into (7), because the curvature in the indentation is much too great to be linked to any local topographic feature, and hence to be described by (3) at all. On the other hand, the shape of the observed, indented path is based on surface temperature, a less reliable indicator of the position of the Stream as a whole than deeper temperatures; the calculated path may actually follow more closely the vertically averaged Stream path than does the "observed" path.

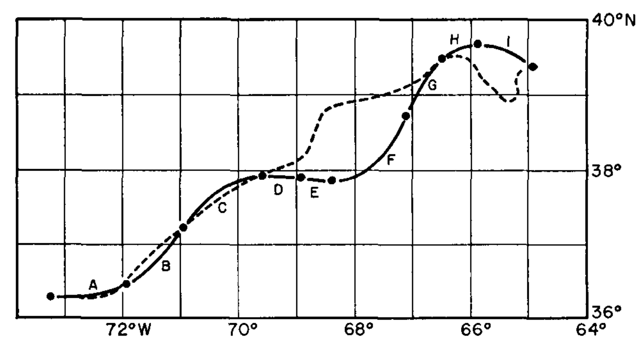

AVERAGE DEPTH GRADIENT FOR EACH PATH SEGMENT:

	D_s	α		D_s	α
A	8×10^{-3}	146°T	F	12×10^{-3}	146°T
B	8×10^{-3}	146	G	12×10^{-3}	135
C	11×10^{-3}	153	H	13×10^{-3}	170
D	11×10^{-3}	153	I	7×10^{-3}	135
E	12×10^{-3}	146			

FIG. 5. Comparison of the Gulf Stream path observed on 24–29 May 1946 with a calculated current path matched to the observed path at its upstream end.

Unlike the other two paths considered, this one overlies the Abyssal Plain only at its downstream end; hence it is not a vanishing of the depth gradient which produced the large anticyclonic meander. Its existence is to be attributed instead to the guiding effect of the northward-turning isobaths between longitudes 66°–65° W. In both the 1948 and 1950 situations, therefore, the sudden, extensive bend in bottom contours is intimately associated with the development of extreme meanders.

Fig. 5 shows the Gulf Stream path found in May 1946 and the corresponding calculated path. The correlation is not so striking as in the previous cases, but is persuasive nevertheless. Since the "observed" path is again actually a surface isotherm, the reservation noted above for the 1948 path should bear on the interpretation of this one also.

The Stream path charted in April 1960 is shown in Fig. 6. For the same reasons given in the discussion of the 1950 paths, the calculated current turns sharply northward just beyond the bend in isobaths, and its path develops another great anticyclonic meander. Since the form of the observed path is based on meridional crossings of the Stream at two degree intervals between longitudes 68°30′ W and 60°30′ W, the

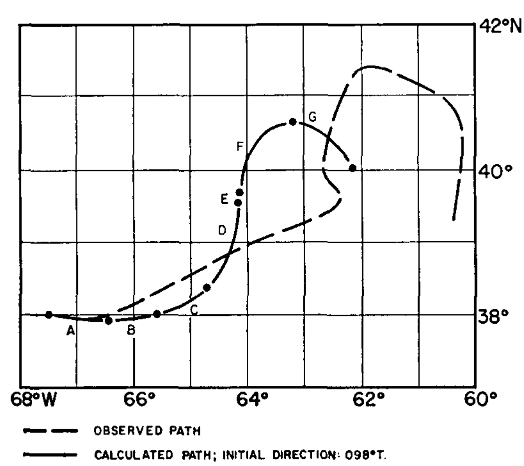

AVERAGE DEPTH GRADIENT FOR EACH PATH SEGMENT:

	D_s	α
A	3×10^{-3}	155°T
B	3×10^{-3}	155
C	6.5×10^{-3}	122
D	0	—
E	7×10^{-3}	165
F	7×10^{-3}	165
G	7×10^{-3}	165

FIG. 6. Comparison of the Gulf Stream path observed in April 1960 with a calculated current path matched to the observed path at its upstream end.

apparent discrepancy between observed and calculated paths on the interval between longitude 66°30′ W and 64°30′ W need not be real.

On the other hand, the calculated central longitude of the anticyclonic meander is much more appropriate to the 1950 meanders than to the one actually seen in 1960, which is located nearly two degrees east of it. This is a real discrepancy, greatly in excess of any encountered in the other comparisons. Furthermore, the path calculations shown in Figs. 2, 3, and 6 were terminated after the large anticyclonic meanders, despite the availability of observational data for downstream comparisons, because of a second discrepancy which would plainly develop. The local meander axes near the downstream ends of these paths are nearly zonal; the symmetry properties of $\eta(\xi)$, implicit in eq. (8), therefore require that the next cyclonic meanders—overlying a level Abyssal Plain—should extend no farther south than the preceding ones. Those actually observed in 1950 and 1960 (shown on Fig. 1), however, clearly reach a good deal farther south than their predecessors; path continuations calculated in the above fashion would hence differ significantly from the observed paths.

The previous successes of the method developed for computations suggest that these discrepancies may not be due to any fundamental error in the underlying mechanism, but perhaps, instead, to a faulty application. A striking topographic feature to which no attention has yet been given is the New England Seamount Arc, located on the Abyssal Plain. (This feature is described by NORTHRUP *et al.*, 1962.) It happens, moreover, that just before developing its great anticyclonic meander, the current path observed in 1960 fairly definitely passes over Kelvin Seamount, centered at 39°00′ N, 63°50′ W. The currents of 1950, on the other hand, seem just to have grazed it, although the path of 8–10 June is somewhat indefinite in this area because no crossing of the current was made between latitudes 38°20′ N and 40°00′ N (F. C. FUGLISTER, private communication). Furthermore, in flowing southward to form the large cyclonic meanders, the currents in both years apparently passed over three additional seamounts in the Arc: San Pablo Seamount, centered at 39°00′ N, 60°40′ W; Manning Seamount, centered at 38°10′ N, 60°50′ W; and Rehoboth Seamount, centered at 37°30′ N, 60°00′ W. One naturally wonders, therefore, whether seamounts might affect ocean currents in some way which would account for disparities in path calculations obtained by treating the Abyssal Plain as everywhere level. Unfortunately, no method is yet apparent for determining the effect of features of seamount-scale on a current like the Gulf Stream; the matter must therefore remain speculative.

It became apparent early in these computations that the calculated current paths were rather sensitive to the directions of the estimated depth gradients; directional deviations, it was found, could easily steer the calculated currents into topographic regimes different from those underlying the corresponding segments of the observed paths. Since the calculated currents would then be subject to topographic effects unlike those which presumably influenced the observed currents, small errors introduced to the computations in this fashion could readily amplify. Unfortunately, the available bathymetric data were sufficiently sparse to permit occasional ambiguities of 10–15° in the directions of estimated depth gradients. Therefore, since the aim in these computations was not to test a method for forecasting positions of the Gulf Stream, but simply to examine the credibility of a particular explanation for observed meander patterns, the error amplification was reduced by adopting that interpretation of the bathymetric data which yielded the best agreement between observed and calculated paths. (It was of course verified that the topographic interpretations made for the five path calculations were consistent with one another.)

Since so few measurements were available for making an estimate of the bottom transport per unit depth, T, the generally close agreement between observed and calculated paths seems at first sight remarkable; one might readily ask whether use of a more accurate, somewhat different value of T would destroy it. The coordinates (ξ, η), however, depend on the bottom transport only through $\sqrt{P}$; that this number is a fraction whose numerator and denominator both depend on deep velocities suggests that it may in fact not be strongly sensitive to the value assigned to T. An expression for P was therefore written in terms of the simple velocity distribution described at the beginning of

Sect. 3. This profile is characterized by two velocities: the cross-stream maximum bottom velocity v_{BM}, and the difference Δv between v_{BM} and the cross-stream maximum surface velocity. The sensitivity of $\sqrt{P}$ to changes in v_{BM} was then calculated as $(v_{BM}/\sqrt{P})(\partial\sqrt{P}/\partial v_{BM})$, where the derivative was taken holding Δv, the depth gradient, and the distance parameters of the profile constant. With the values cited in Sect. 3 for the relevant variables, and with $D_x = 4 \times 10^{-3}$, $D_y = 7 \times 10^{-3}$, the sensitivity turned out to be 0.2. This result may be interpreted by noting that if the sensitivity were independent of v_{BM}—as it is not—a 50 % change in v_{BM} would induce a change in $\sqrt{P}$, and hence in calculated values of ξ and η, of only 10 %. For this velocity distribution, $\sqrt{P}$ is thus not very sensitive to variations in bottom velocity, at least in the neighborhood of the particular numbers descriptive of the profile. One is encouraged to believe, therefore, that the generally close agreement between observed and calculated current paths is not fortuitous, but is, instead, convincing evidence for topographic control.

The amplification by varying topography of deviations between calculated current paths suggests a partial explanation for the great diversity in observed meander patterns. Since bottom topography is fixed, time changes in current paths described by (7) must be associated with changes in initial conditions. Since the Gulf Stream leaves the vicinity of the Continental Slope and enters the open ocean just as it passes Cape Hatteras, it should be governed by eq. (3) at least that far upstream, so that the appropriate "initial" conditions for the topographically controlled Stream must be its direction and path curvature near Hatteras. Changes produced somehow in these characteristics would not only change the shape of the wave described by (7), but also direct the Stream into topographic regimes different from those underlying it at an earlier time; it would then be subject to different deflective tendencies, and hence follow a course perhaps quite different from that taken earlier. Thus, although the topography at a fixed point cannot change with time, variations in current direction and path curvature would cause time changes in the effective topography influencing the Stream; these in turn would transform the initial variations into major alterations in meander patterns downstream. That directional variations of some sort do in fact occur at Hatteras is amply indicated by the well established fluctuations in current direction and position off Onslow Bay (von Arx, *et al.*, 1955; Webster, 1961*b*).

To test the premise of this explanation, we may ascertain how well the calculated paths of Fig. 2–6, if extended upstream according to the solution of (7), converge on Cape Hatteras, the "source" of the open-ocean Gulf Stream; poor convergence would make doubtful the upstream existence of topographic control. Even a cursory inspection of the distribution of isobaths shows that topographically controlled currents passing through the initial points of the previous calculations must stem from the general Hatteras area. Upstream path extensions have been calculated, moreover, and are displayed in Fig. 7. The points farthest downstream on each segment are the initial points of the corresponding calculated paths discussed above; the computations were carried out upstream from these points and terminated at inflection points near Hatteras. The relevant topographic data are presented in the table following. Clearly the convergence of the several path extensions is very close, and sustains the interpretation of the observed Gulf Stream paths as segments of a topographically controlled current "originating" in proximity to the Continental Slope near Cape Hatteras.

6. Concluding remarks

It is assumed in this study that the portion of the Gulf Stream overlying the Continental Rise is a flow sufficiently concentrated and intense for it to be assigned lateral boundaries, albeit in a crude and not clearly specified manner; and that the flow is vertically coherent, roughly to the extent that vertical variations in the position of the Stream are smaller than its width. No attempt is made to deduce such a current from physical principles and oceanic boundary conditions; rather, its existence is taken as empirically established. It then makes fair sense to characterize the Stream as a whole by a single curve: a current path. It is further assumed, on the basis of recent observations, that the flow persists to the bottom of the ocean, without reversing direction.

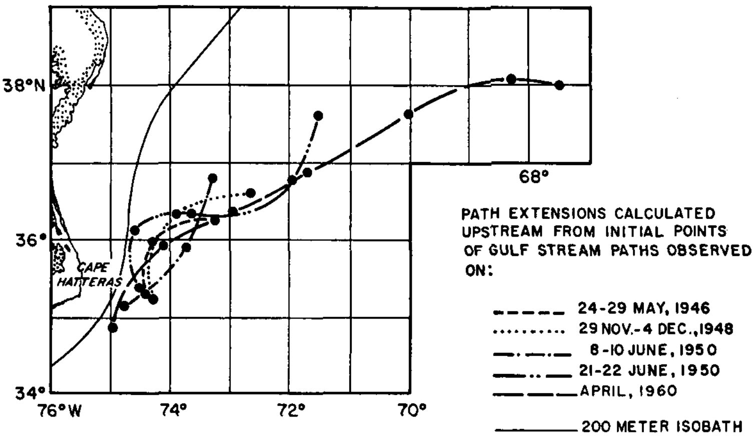

FIG. 7. Upstream extensions of calculated current paths.

Analysis on this basis of the magnitudes and scales of gross motions in the Gulf Stream, as estimated at present, suggests that current paths are determined essentially by a steady-state response principally to variations in ocean depth, and, in a lesser degree, to the meridional variation in Coriolis parameter. Furthermore, approximate descriptions of current paths governed by this mechanism (conservation of potential vorticity) fit observed path segments so closely as to make very convincing the interpretation of the large-scale meanders as segments of combined topographic and Rossby waves. This interpretation explains fully the similarity between the trends of deep isobaths and observed current paths, the tendency of the Stream to form large anticyclonic meanders just downstream from the great northward turn in bottom contours, and the correlation between the amplitudes of these meanders and the positions of the underlying isobaths. It is suggested that the apparently slow time variations in meander patterns are associated with changes in current direction and path curvature near Cape Hatteras, but no attempt is made to describe evolutions of the Stream path from one pattern to another.

No doubt the least firmly established feature of this conception of the Stream is the persistence to the bottom of the ocean of flow in the same direction as the surface current. The only reliable measurements made to date of

TABLE 1. *Depth gradients used for path-extension calculations.*

Successive gradients for each interval between adjacent calculated points are given in upstream order. Paths are identified by the dates of the end-point observations.

24–29 May 1946	29 Nov.–4 Dec. 1948	8–10 June 1950	21–22 June 1950	April 1960
$D_s = 14 \times 10^{-3}$ $\alpha = 120°T$	$D_s = 9 \times 10^{-3}$ $\alpha = 130°T$	$D_s = 11 \times 10^{-3}$ $\alpha = 112°T$	$D_s = 12 \times 10^{-3}$ $\alpha = 120°T$	$D_s = 7 \times 10^{-3}$ $\alpha = 165°T$
$D_s = 21 \times 10^{-3}$ $\alpha = 122°T$	$D_s = 21 \times 10^{-3}$ $\alpha = 108°T$	$D_s = 15 \times 10^{-3}$ $\alpha = 124°T$	$D_s = 8 \times 10^{-3}$ $\alpha = 140°T$	$D_s = 10 \times 10^{-3}$ $\alpha = 165°T$
			$D_s = 19 \times 10^{-3}$ $\alpha = 120°T$	$D_s = 3 \times 10^{-3}$ $\alpha = 135°T$
			$D_s = 19 \times 10^{-3}$ $\alpha = 120°T$	$D_s = 8 \times 10^{-3}$ $\alpha = 146°T$
				$D_s = 9 \times 10^{-3}$ $\alpha = 130°T$
				$D_s = 20 \times 10^{-3}$ $\alpha = 120°T$

deep motions beneath the relevant portions of the surface Stream consist of the few observations in 1960 with neutrally buoyant floats. Should these results turn out not to be at all typical of the Stream, the topographic explanation of meanders would fail. On the other hand, the close agreement between calculated and observed current paths, achieved by assuming bottom velocities as implied by the 1960 measurements, constitutes a fairly compelling argument for such a flow being generally a property of the Stream.

No attention has been given here to possible instabilities of the Gulf Stream. According to the idea of topographic control, interpretations of the large-scale meanders as self-amplified perturbations to some rectilinear equilibrium flow seem to have proceeded, in a sense, from a misconception: the topography of the Continental Rise is so irregular that any synoptic current which extends to the bottom of the ocean must necessarily meander; a rectilinear equilibrium current is impossible. Apparently the very meanders which have been construed as unstable disturbances to some basic flow ought properly to be regarded as intrinsic features of the basic flow itself. It is conceivable that features of a smaller scale, e.g. the indentation of the large anticyclonic meander in Fig. 4, may turn out to be linked to an instability, but they would then be treated as disturbances to an initially meandering basic current. It seems also possible that instabilities in the Stream south of Cape Hatteras might account for the fluctuations in current direction and path curvature near Hatteras to which we have attributed the diversity in observed meander patterns, but instability would then have at most an indirect influence on the meanders downstream.

Since meanders, and hence path curvature, tend to be averaged out of mean currents, we should expect, on a rough mean basis, to find the net northward advection of planetary vorticity in the Gulf Stream east of Cape Hatteras to be balanced topographically by a gradual increase in ocean depth beneath the Stream. Thus the mean axis of the Gulf Stream, as estimated on U.S. Navy Hydrographic Office Chart No. 1412 (and reproduced in ISELIN and FUGLISTER, 1948), traces a rectilinear path between Cape Hatteras and longitude 72° W, with an implied current set of 043° T. The underlying isobaths are nearly rectilinear, and are characterized by a depth gradient of magnitude 8×10^{-3} and direction 125° T. According to eqs. (8) and (9), for values of the current parameters V, M, T, the same as above, the associated current determined entirely by a balance between topographic and β-effects must be rectilinear with bearing 045° T. This agreement between directions of the mean and calculated rectilinear currents confirms the expected mean vorticity balance, although the closeness of agreement may be partly fortuitous.

Topographic domination of the Gulf Stream vorticity balance must make doubtful the explanation recently proposed by CARRIER and ROBINSON (1962) for the separation of the Stream from the coast after it passes Cape Hatteras. They considered oceanic circulations forced by a meridionally-varying zonal wind stress, and deduced an eastward inertial jet at the latitude of maximum wind-stress curl. They suggested that the abrupt change in direction as the current entered the mid-latitude jet represented the separation of Stream from coast near Cape Hatteras. The fundamental conclusion of the present study, however, is that the path of the Stream, after it passes Cape Hatteras, is controlled for some considerable distance principally by bottom topography, and thus not by the distribution of wind stress. In particular, the mean axis of the Stream does not actually change direction until some 300 km downstream from Hatteras, at a point where the deep isobaths also bend sharply. That the Gulf Stream should abruptly turn eastward seems therefore not to be an element of the separation problem, but simply a consequence of the topographic constraint.

Acknowledgements

I am indebted to Mr. F. C. Fuglister for very considerable instruction concerning the character of the Gulf Stream, and for permission to use unpublished results of his Gulf Stream survey of 1960; to Dr. T. F. Webster for many helpful discussions; and to Dr. W. S. von Arx for critical comment. I should like to acknowledge support from the Woods Hole Oceanographic Institution in the form of fellowships, and support by the Office of Naval Research, under contract Nonr-2196(01).

REFERENCES

CARRIER, G. F., and ROBINSON, A. R., 1962, On the theory of the wind-driven ocean circulation. *J. Fluid Mech.*, **12**, 1, pp. 49–80.

FORD, W. L., and MILLER, A. R., 1952, The surface layer of the Gulf Stream and adjacent waters. *J. Marine Res.*, **11**, 3, pp. 267–280.

FUGLISTER, F. C., 1960, *Atlantic Ocean Atlas of Temperature and Salinity Profiles and Data from the International Geophysical Year of* **1957–1958**. Woods Hole Oceanographic Institution, 209 pp.

FUGLISTER, F. C., Gulf Stream '60. In *Progress in Oceanography*, Vol. 1. Pergamon Press, London, New York. (in press).

FUGLISTER, F. C., and WORTHINGTON, V., 1947, Meanders and velocities of the Gulf Stream. *Woods Hole Oceanographic Institution, Tech. Rep. No. 9 on the Hydrography of the Western Atlantic* (unpublished manuscript).

FUGLISTER, F. C., and WORTHINGTON, L. V., 1951, Some results of a multiple ship survey of the Gulf Stream. *Tellus*, **3**, 1, pp. 1–14.

HAURWITZ, B., and PANOFSKY, H. A., 1950, Stability and meandering of the Gulf Stream. *Trans. Amer. Geophys. Union*, **3**, 5, pp. 723–731.

ISELIN, C. O'D., 1936, A study of the circulation of the western North Atlantic. *Pap. Phys. Oceanogr. and Meteor.*, **4**, 4, 101 pp.

ISELIN, C. O'D., and FUGLISTER, F. C., 1948, Some recent developments in the study of the Gulf Stream. *J. Marine Res.*, **7**, 3, pp. 317–329.

NEUMANN, G., 1956, Notes on the horizontal circulation of ocean currents. *Bull. Amer. Meteor. Soc.*, **37**, 3, pp. 96–100.

NORTHRUP, J., FROSCH, R. A., and FRASSETO, R., 1962, Bermuda–New England Seamount Arc. *Geol. Soc. America Bull.*, **73**, 5, pp. 587–594.

ROSSBY, C.-G., 1940, Planetary flow patterns in the atmosphere. *Quart. J. Roy. Meteor. Soc.*, **66**, Suppl., pp. 68–87.

STERN, M. E., 1961, The stability of thermoclinic jets. *Tellus*, **13**, 4, pp. 503–508.

STOMMEL, H., 1955, Lateral eddy viscosity in the Gulf Stream System. *Deep-Sea Res.*, **3**, 1, pp. 88–90.

STOMMEL, H., 1958, *The Gulf Stream.* Univ. of California Press, Berkeley, 202 pp.

VON ARX, W. S., 1960, The line of zero set. *Deep-Sea Res.*, **7**, 3, pp. 219–220.

VON ARX, W. S., BUMPUS, D. F., and RICHARDSON, W. S., 1955, On the fine structure of the Gulf Stream front. *Deep-Sea Res.*, **3**, 1, pp. 46–65.

WARREN, B. A., 1962, Topographic influences on the path of the Gulf Stream. Doctoral Dissert., Dept. of Geology and Geophysics, M.I.T. (unpublished manuscript).

WEBSTER, F., 1961*a*, The effect of meanders on the kinetic energy balance of the Gulf Stream. *Tellus*, **12**, 3, pp. 392–401.

WEBSTER, F., 1961*b*, A description of Gulf Stream meanders off Onslow Bay. *Deep-Sea Res.*, **8**, 2, pp. 130–143.